DOI: 10.1002/cbic.200700579

Direct Evidence for ArO—S Bond Cleavage upon Inactivation of *Pseudomonas aeruginosa* Arylsulfatase by Aryl Sulfamates

Pavla Bojarová,[a] Emma Denehy,[a] Ian Walker,[a] Karen Loft,[a] David P. De Souza,[b] L. W. Lawrence Woo,[c] Barry V. L. Potter,[c] Malcolm J. McConville,[b] and Spencer J. Williams*[a]

Pseudomonas aeruginosa *arylsulfatase catalyses the cleavage of aryl sulfates and is an excellent model for human estrone sulfatase, which is implicated in hormone-dependent breast cancer. Aryl sulfamates are inactivators of sulfatases; however, little is known about their mechanism. We studied the inactivation of* Pseudomonas aeruginosa *arylsulfatase* A *by a range of aryl sulfamates, including the clinical agent 667COUMATE (STX64) used to inactivate estrone sulfatase. Inactivation was time dependent, irreversible, and active-site directed, consistent with a covalent modification at the active site. In terms of the kinetic parameters of inactivation* k_{inact} *and* K_i, K_i *values are in the micromolar to nanomolar range, and the inactivation half-life is less than 30 s. A Brønsted plot of* k_{inact}/K_i *has a steep slope* ($\beta_{lg} = -1.1$), *which implies that the transition state for the first irreversible chemical step of inactivation involves a high degree of charge transfer and cleavage of the ArO–S bond. Detection of the released phenol and titration of the residual activity showed the stoichiometry of inactivation to be in the range 3–6, with the greatest values found for the most effective inactivators. Thus, multiple sulfamoylation events appear to occur during the inactivation process. These data provide valuable insight into the mechanism of sulfatase inactivation by sulfamates.*

Introduction

The enzymes that cleave sulfate esters, sulfatases (EC 3.6.1.-), have important roles in human health and disease.[1–3] Estrone sulfatase has been implicated in the progression of breast cancer in postmenopausal women,[4,5] and other sulfatases participate in mechanisms of bacterial pathogenesis[6,7] and the evasion of plant defence mechanisms against insect pests.[8] Therefore, the design of sulfatase inhibitors attracts considerable attention, both for the study of the effects of sulfatase dysfunction and for therapeutic interventions. The most promising inhibitors of sulfatases are esters of sulfamic acid, H_2NSO_2OH, such as EMATE,[9] COUMATE,[10] and 667COUMATE[11] (Scheme 1). 667COUMATE (also known as STX64, BN83495), an inactivator of estrone sulfatase, has entered clinical trials for the treatment of hormone-dependent breast cancer.[12] Despite the potent inhibition of sulfatases caused by sulfamates, little is known about the mechanism of inactivation. One of the reasons is that most studies have been performed with human placental arylsulfatase, a membrane-associated enzyme that is difficult to acquire in the quantities and purity necessary for a detailed mechanistic investigation.

Pseudomonas aeruginosa arylsulfatase A (*Pa*AtsA) is a bacterial sulfatase that catalyses the hydrolysis of a diverse range of aryl sulfate esters.[13] Like all sulfatases, *Pa*AtsA possesses a post-translational modification, whereby an active-site cysteine residue has been converted into formylglycine (FGly).[14] In eukaryotes, this conversion is mediated by formylglycine-generating enzyme (FGE).[15] In some prokaryotes, this modification is formed by the oxidation of an active-site serine residue by the iron–sulfur protein AtsB.[16] Remarkably, *E. coli*, although it does not possess an active sulfatase, is capable of effecting the

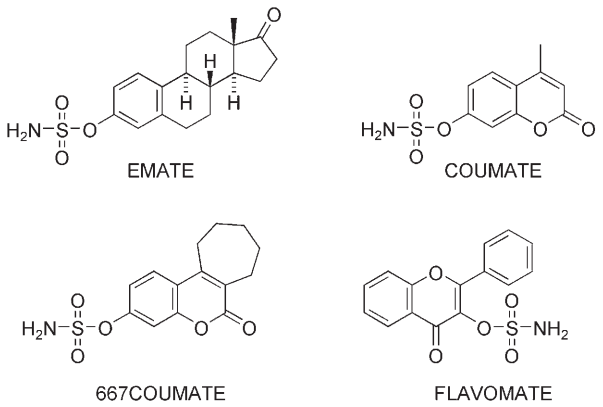

Scheme 1. Examples of aryl sulfamate inactivators of sulfatases.

[a] *Dr. P. Bojarová, E. Denehy, Dr. I. Walker, K. Loft, Dr. S. J. Williams*
School of Chemistry and Bio21 Molecular Science and Biotechnology Institute, University of Melbourne
30 Flemington Road, 3010 Parkville, Victoria (Australia)
Fax: (+61) 3-9347-8124
E-mail: sjwill@unimelb.edu.au

[b] *D. P. De Souza, Prof. M. J. McConville*
Department of Biochemistry and Molecular Biology
University of Melbourne
30 Flemington Road, 3010 Parkville, Victoria (Australia)

[c] *Dr. L. W. L. Woo, Prof. B. V. L. Potter*
Department of Pharmacy and Pharmacology, University of Bath
Claverton Down, Bath BA2 7AY (UK)

Supporting information for this article is available on the WWW under http://www.chembiochem.org or from the author.

post-translational modification of the active-site cysteine residue of *Pa*AtsA to FGly. *Pa*AtsA is therefore an excellent model for the study of human estrone sulfatase, as it can be acquired in large amounts in homogeneous form by recombinant expression in *E. coli*. Furthermore, *Pa*AtsA shares considerable sequence similarity with all known sulfatases, and its three-dimensional X-ray crystal structure shows the same fold and active-site architecture as that of human estrone sulfatase.[3,14,17] Very recently, sulfamates were shown to effect the time-dependent inactivation of *Pa*AtsA.[18] This finding has provided an opportunity to gain insight into the mechanism of sulfatase inactivation by sulfamates through the study of this readily acquired enzyme.

Three different mechanisms of catalysis by sulfatases have been suggested that involve the active-site FGly residue (Scheme 2). The first proposes that hydrolysis is initiated by the addition of the sulfate ester substrate to the aldehyde of FGly; the attack of the resulting intermediate at the sulfur atom by water liberates the parent alcohol of the sulfate ester and leaves the sulfate moiety bound to the enzyme; the elimination of hydrogen sulfate to regenerate FGly completes the cycle (Scheme 2A).[19] The second mechanism proposes that the FGly residue is first hydrated to form a geminal diol; next, one of the geminal hydroxy groups attacks the sulfur atom of the sulfate ester to expel the parent alcohol and give a covalently sulfated enzyme intermediate; finally, the elimination of sulfate completes the catalytic cycle (Scheme 2B).[20] The third alternative predicts a different fate for the enzyme sulfate intermediate formed in either of the two mechanisms proposed above; elimination occurs by loss of the α proton on the FGly residue to form an enol; this enol tautomerises to regenerate the active-site aldehyde (Scheme 2C).[21] Although some have argued for the involvement of the geminal hydrate of FGly as an enzyme nucleophile on the basis of X-ray crystal structures in which this species was observed,[20,22] no definitive evidence has yet been presented to allow a clear-cut distinction between any of these mechanistic alternatives.

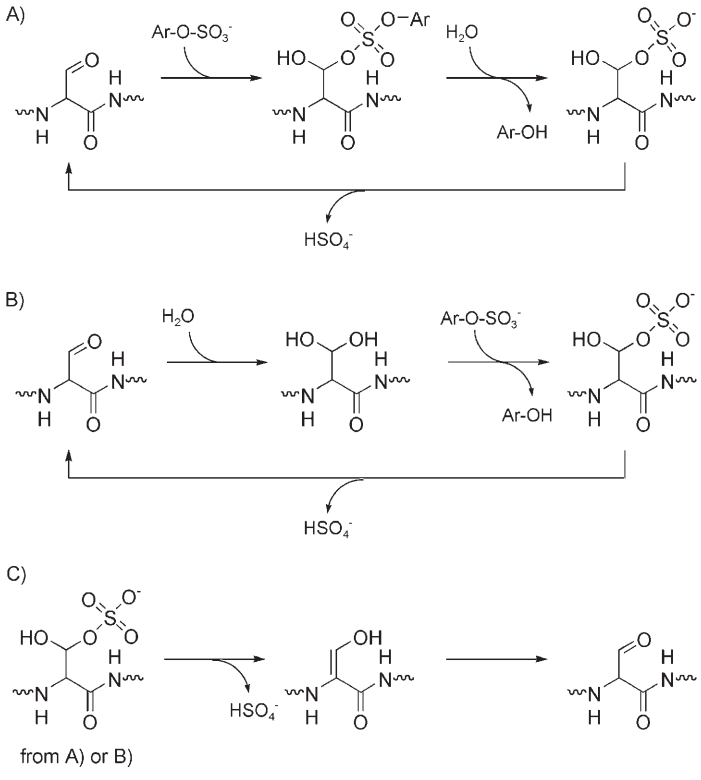

Scheme 2. Three possible mechanisms involving the active-site FGly residue for the cleavage of sulfate esters catalysed by sulfatases.

Aryl sulfamates exhibit potent, time-dependent inhibition of sulfatases. Enzyme activity is not recovered even after the removal of excess inactivator,[9,18,23] and the presence of a substrate protects against inactivation.[9,18] These data are consistent with an inactivation mechanism that involves covalent modification of the active site. However, despite intensive study over many years, the identity of this modification has remained elusive.[11,18]

The importance of sulfamates as inactivators of sulfatases, and the uncertainty of their mechanism of action, prompted us to investigate their inactivation of *Pa*AtsA. We synthesised a range of substituted aryl sulfamates and studied the kinetics of *Pa*AtsA inactivation. A linear free-energy plot revealed that the efficiency of inactivation, expressed as the ratio k_{inact}/K_i, is dependent upon the pK_a value of the parent phenol of the aryl sulfamate and thus provided the first unequivocal evidence that inactivation occurs through the cleavage of the ArO–S bond. Further evidence for the cleavage of this bond during the inactivation process was obtained by the direct detection of the phenol released upon inactivation. Finally, we determined the stoichiometry of the inactivation of *Pa*AtsA by several sulfamates, including 667COUMATE. These studies present fundamental details on the bond-breaking steps that occur during the inactivation of sulfatases by sulfamates and give new insight into the mechanism of inactivation.

Results

Expression and kinetic analysis of *Pa*AtsA

*Pa*AtsA[13] was expressed as a C-terminal pET30 His_6-tagged construct in *E. coli* BL21(λDE3) and purified by affinity chromatography on Ni-NTA resin and hydrophobic chromatography on *tert*-butyl Sepharose. The substrate potassium 4-methoxyphenyl sulfate (**1**) was prepared as reported previously,[24] and potassium 4-methylumbelliferyl sulfate (**2**) was prepared as outlined in the Supporting Information. Kinetic parameters for the hydrolysis of substrates **1** and **2** by *Pa*AtsA under various conditions are shown in Table 1. The low K_i values of many of the aryl sulfamates investigated required the use of the enzyme at a nanomolar concentration to ensure that the concentration of the inactivator did not change during inactivation (i.e., $[I] \gg [E]_0$).[25] In such demanding cases, we preferred the fluorometric assay with substrate **2**. This assay was at least 100-fold more sensitive than the spectrophotometric assay with substrate **1**.

Table 1. Michaelis–Menten parameters for the *Pa*AtsA-catalysed hydrolysis of selected substrates under various conditions.

Substrate[a]	Assay medium[b]	k_{cat} [s^{-1}]	K_m [μM]	k_{cat}/K_m [$s^{-1}\,\mu M^{-1}$]
1	pH 9	72±2	310±30	0.23±0.03
1	pH 7	16.2±0.5	42±5	0.39±0.05
1	pH 7, 5% EtOH	8.0±0.2	41±4	0.19±0.02
2	pH 9	82±1	12.2±0.6	6.7±0.3

[a] **1** is potassium 4-methoxyphenyl sulfate, **2** is potassium 4-methylumbelliferone sulfate. [b] Assays were performed at 37 °C in 25 mM bis-tris propane/25 mM glycine/0.05% BSA buffer at the pH value indicated. The enzyme concentration was determined by GC/MS analysis.

Determination of the concentration of *Pa*AtsA and the degree of post-translational modification

The concentration of purified *Pa*AtsA was determined by GC/MS to be 65±11 μM (see the Supporting Information). Coincidentally, this value compares well with that derived from a BCA protein assay (Pierce Biotechnology; 60±5 μM with a BSA standard). An extinction coefficient of $\varepsilon_{280}=(1.7\pm0.3)\times10^5\,M^{-1}\,cm^{-1}$ was calculated for the enzyme on the basis of the experimentally determined enzyme concentration. Quantification of the degree of post-translational modification is particularly important, as this modification to FGly is vital for sulfatase activity.[26,27] As the sequence for *Pa*AtsA encodes only a single cysteine residue, Cys51, the degree of post-translational modification to FGly may be assayed conveniently by using the Ellman reagent (5,5′-dithiobis(2-nitrobenzoic acid)) under denaturing conditions (4 M guanidine hydrochloride), to ensure exposure of the cysteine residue to this reagent. This assay revealed that 97% of the Cys residues of *Pa*AtsA were modified to FGly.

pH dependence of *Pa*AtsA activity

The analysis of *Pa*AtsA activity with substrate **1** revealed a bell-shaped dependence of the kinetic parameters on the pH value (Figure 1), with the maximum catalytic activity (k_{cat}/K_m) at pH 7.9. This profile indicates that the catalytic activity is determined by the ionisation of two active-site residues, of pK_a value 7.1±0.2 for the acidic limb and 8.7±0.1 for the basic limb. The pH profile of k_{cat} increases to a maximum at high pH values, and thus mirrors that of K_m. As *Pa*AtsA is unstable below pH 5, the acidic limb of the profile could not be fully defined. Similarly, as *Pa*AtsA is unstable above pH 10, the maxima for the parameters k_{cat} and K_m could not be accurately determined.

Aryl sulfamates are active-site-directed inactivators of *Pa*AtsA

Ten substituted aryl sulfamates, **3**–**12** (Figure 2), were synthesised as described previously.[24] The results of elemental analysis were satisfactory (±0.4%) for all new compounds and those used for active-site-titration experiments (see the Supporting Information). At pH 7, the spontaneous rate of hydrolysis of 4-nitrophenyl sulfamate (**3**; pK_a value of 4-nitrophenol: 7.15) was too high (decay rate constant, $k_{uncat}=0.084\ min^{-1}$) for the accurate measurement of inactivation kinetics. In fact, only sulfamates with p$K_a\geq8$ for the parent phenol were sufficiently stable ($k_{uncat}<0.005\ min^{-1}$) at pH 7 for kinetic studies. For our purposes, the activity and stability of *Pa*AtsA were satisfactory in the range pH 5–9, and the maximum assay sensitivity was observed at pH 9. Thus, all inactivation studies were carried out at a pH value within this range. After incubation with the inactivator at a selected pH value, the residual enzyme activity was determined at pH 9.

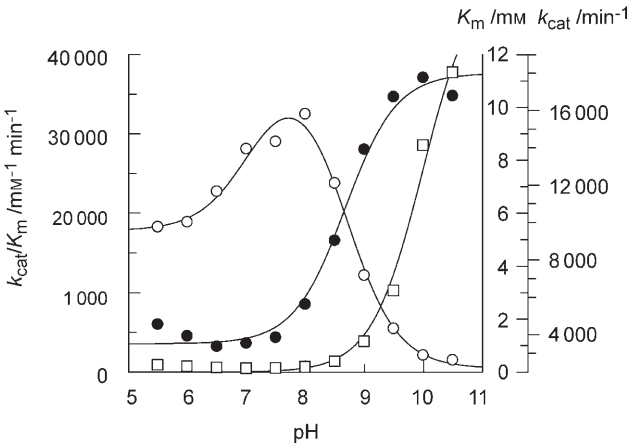

Figure 1. pH profile of *Pa*AtsA catalytic activity. The pH profile was measured with potassium 4-methoxyphenyl sulfate (**1**) as the substrate: ●: k_{cat}, □: K_m, ○: k_{cat}/K_m.

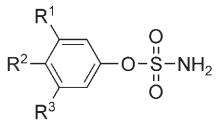

Compound	pK_a	R^1	R^2	R^3
3	7.15	H	-NO_2	H
4	7.97	H	-CN	H
5	8.18	Cl	H	Cl
6	8.36	-NO_2	H	H
7	8.61	-CN	H	H
8	9.12	Cl	H	H
9	9.21	H	I	H
10	9.41	H	Cl	H
11	9.99	H	H	H
12	10.10	H	-OCH_3	H

Figure 2. Structures of aryl sulfamates **3**–**12** and the corresponding pK_a value of the parent phenol.

Inactivation kinetics were assessed according to Equation (1), in which E, I, and E–P are the enzyme, aryl sulfamate, and covalent adduct, respectively, K_i is the dissociation constant for the enzyme–sulfamate complex, and k_{inact} is the first-order rate constant for the conversion of the noncovalent E·I complex into the E–P complex:

$$E + I \overset{K_i}{\rightleftharpoons} E\cdot I \xrightarrow{k_{inact}} E\text{-}P \qquad (1)$$

Many of the sulfamates demonstrated limited water solubility and were therefore used as stock solutions in EtOH. The final concentration of EtOH in the inactivation mixtures was 5%. The presence of 5% EtOH resulted in a reversible decrease in enzyme activity by decreasing the value of k_{cat}. However, this effect was of little consequence, as the dilution of inactivation mixtures containing 5% EtOH into a buffer at pH 9 containing the substrate, to measure residual activity, resulted in the complete recovery of enzyme activity (data not shown).

The ability of sulfamates to cause active-site-directed, time-dependent, and irreversible inactivation of *Pa*AtsA was first investigated with phenyl sulfamate (**11**; pK_a value of phenol: 9.99). Compound **11** is stable at a range of pH values (at pH 5–9, $k_{uncat} = 2 \times 10^{-4}$ min^{-1}). At pH 7 and 9, inactivation by **11** (20 μM) was both time-dependent and irreversible, with no recovery of activity of the inactivated enzyme after removal of excess free inactivator by dialysis. The inactivation of *Pa*AtsA by compound **11**, and by all other inactivators studied, followed first-order kinetics. Full kinetic analysis of the inactivation of *Pa*AtsA by **11** revealed it to be an effective inhibitor (Table 2; $K_i = 18 \pm 3$ μM, $k_{inact} = 0.057 \pm 0.004$ s^{-1}, $k_{inact}/K_i = 0.0031 \pm 0.0005$ s^{-1} μM^{-1} at pH 9). By contrast, at pH 5, no time-dependent inactivation by **11** was observed. When the enzyme inactivated at pH 7 was purified to remove excess inactivator and incubated at pH 5, no reactivation occurred. These results demonstrate that $k_{inact} = 0$ at pH 5, and that the inactivated complex, E–P, is not reactivated at pH 5–9.

To demonstrate that sulfamates cause active-site-directed inactivation of *Pa*AtsA, we sought a competitive inhibitor of *Pa*AtsA. Sodium tetraborate[28] was found to act as a purely competitive inhibitor of *Pa*AtsA at pH 9 (37 °C) with $K_c = 178 \pm 14$ μM (Figure 3A); interestingly, at pH 7, sodium tetraborate causes mixed inhibition of *Pa*AtsA. Sodium tetraborate protected *Pa*AtsA against inactivation by **11** at pH 9 in a concentra-

Table 2. Inactivation parameters for the inhibition of *Pa*AtsA by aryl sulfamates **4**–**12**, COUMATE, 667COUMATE, and FLAVOMATE.

Inactivator[a]	pK_a[b]	k_{uncat} [min^{-1}][c]	k_{inact} [s^{-1}]	K_i [μM]	$t_{1/2}$ [s]	k_{inact}/K_i [s^{-1} μM^{-1}]
4	7.97	0.0030	0.1 ± 0.02	0.092 ± 0.034	7.2	1.1 ± 0.4
5	8.18	n.d.[e]	0.08 ± 0.01	0.094 ± 0.026	8.4	0.87 ± 0.3
6	8.36	n.d.[e]	0.063 ± 0.007	0.13 ± 0.03	11	0.48 ± 0.1
7	8.61	n.d.[e]	0.059 ± 0.005	0.28 ± 0.06	12	0.21 ± 0.05
8	9.12	n.d.[e]	0.045 ± 0.002	0.16 ± 0.03	15	0.28 ± 0.05
9	9.21	n.d.[e]	0.059 ± 0.004	0.19 ± 0.03	12	0.31 ± 0.05
10	9.41	n.d.[e]	0.049 ± 0.003	0.64 ± 0.1	14	0.08 ± 0.01
11	9.99	0.0002	0.034 ± 0.001	7.9 ± 0.9	22	0.0043 ± 0.0005
11[d]	9.99	0.0002[d]	0.057 ± 0.004	18 ± 3	12	0.0031 ± 0.0005
12	10.10	n.d.[e]	0.026 ± 0.001	7.6 ± 1.3	27	0.0034 ± 0.0006
COUMATE	7.8[34]	0.0048	0.079 ± 0.008	0.076 ± 0.019	8.8	1.0 ± 0.3
667COUMATE	9.1[10]	n.d.[e]	0.18 ± 0.04	0.24 ± 0.08	3.9	0.74 ± 0.3
FLAVOMATE	9.8[35]	0.0034	> 0.1	< 0.05	n.d.[e]	> 2

[a] Unless otherwise stated, inactivation experiments were performed at 37 °C in 25 mM bis-tris propane/25 mM glycine buffer at pH 7 with 0.05% BSA and 5% EtOH (enzyme concentration: 9 nM) and assayed fluorometrically with **2** (30 μM) as the substrate. [b] The pK_a values of the parent phenols were taken from ref. [36]. [c] The decay of the sulfamates was assayed under inactivation conditions. [d] Inactivation and decay were assayed at pH 9. [e] Not determined.

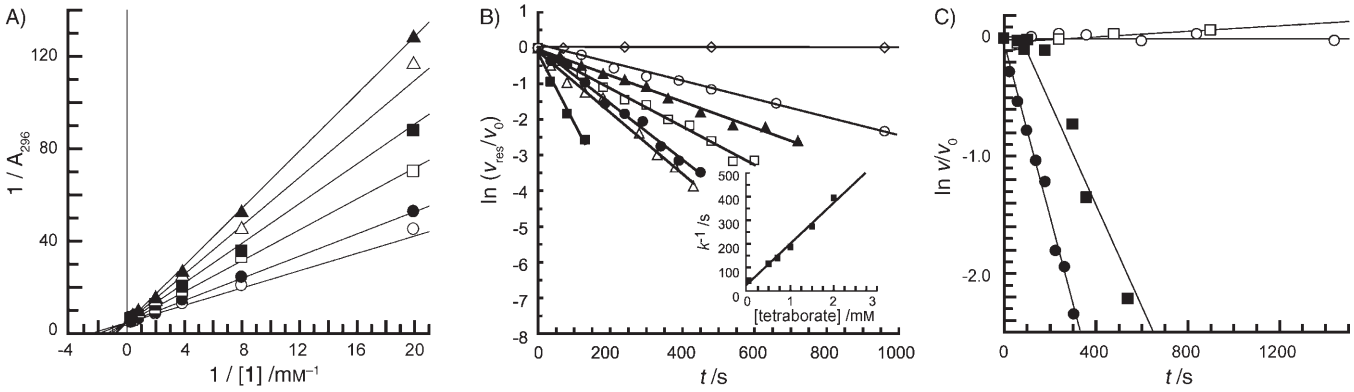

Figure 3. A, B) Sodium tetraborate protects *Pa*AtsA against inactivation by phenyl sulfamate (**11**). A) Lineweaver–Burk plot of the hydrolysis of substrate **1** at increasing concentrations of sodium tetraborate (pH 9, 37 °C). The intersection of the plots at the *y* axis at $1/k_{cat}$ at all sodium tetraborate concentrations demonstrates competitive inhibition. Concentration of sodium tetraborate: 0 (○), 50 (●), 140 (□), 230 (■), 320 (△), 410 mM (▲). B) Semilogarithmic plot of the inactivation of *Pa*AtsA by **11** (20 μM) in the presence of sodium tetraborate (0–2 mM) at pH 9. Concentration of sodium tetraborate: 2 (○), 1.5 (▲), 1 (□), 0.7 (●), 0.5 (△), 0 mM (■); control: ◇. Inset: Plot of the inverse pseudo-first-order rate constant of inactivation (k^{-1}) against the concentration of sodium tetraborate. C) The substrate protects *Pa*AtsA against inactivation by **11** at pH 7. Inactivation mixtures contained **11** (20 μM) and **1** (0 (●), 1 (■), or 80 mM (□)); control reaction in the absence of an inactivator: ○.

tion-dependent manner (Figure 3B). This result is consistent with the competition of sodium tetraborate with the free inactivator according to Equation (2), in which I_c is tetraborate, and K_c is the dissociation constant for the complex of the enzyme with this competitive inhibitor:

$$\begin{array}{l} E + I \underset{}{\overset{K_i}{\rightleftharpoons}} E\cdot I \xrightarrow{k_{inact}} E\text{-}P \\ + \\ I_C \\ \Big\| K_c \\ E\cdot I_C \end{array} \qquad (2)$$

A plot of the inverse pseudo-first-order rate constant, k^{-1}, against the concentration of sodium tetraborate enabled the determination of the inhibition constant for phenyl sulfamate (**11**) at pH 9: $K_i = 10\ \mu M$. This value compares favourably with that measured by full kinetic analysis (Table 2). As sodium tetraborate exhibits mixed inhibition at pH 7, the active-site-directed nature of inactivation at pH 7 was demonstrated unambiguously by the protection by substrate **1** of *Pa*AtsA against inactivation with **11** (Figure 3C).

Brønsted dependence of *Pa*AtsA inactivation

We studied the inactivation of *Pa*AtsA by nine aryl sulfamates, **4**–**12** (pK_a values of the parent phenols: 7.97–10.10), by using substrate **2**. For all inactivators studied, the inactivation obeyed saturable kinetics,[25] which allowed the extraction of k_{inact} and K_i values (Table 2). All compounds studied were outstandingly efficient inactivators with K_i values in the nano- to micromolar range and an inactivation half-life, $t_{1/2}$, of 7–30 s at saturating concentrations. Inactivation occurred at such high rates that the fastest inactivators, compounds **4** and **5**, could not be assayed at saturating concentrations. A Brønsted plot (Figure 4) of $\log k_{inact}/K_i$ against the pK_a value of the parent phenol showed a linear dependence and a slope of close to unity ($\beta_{lg} = -1.1 \pm 0.2$).

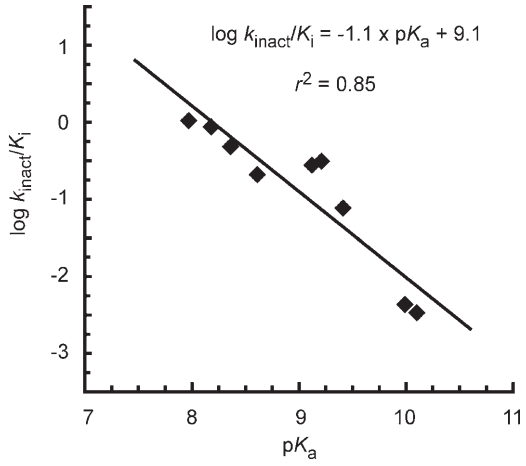

Figure 4. A Brønsted plot of inactivation efficiency (k_{inact}/K_i) reveals significant charge development at the transition state for inactivation. Dependence of the logarithm of the second-order rate constant, k_{inact}/K_i, for the inactivation of *Pa*AtsA by aryl sulfamates **4**–**12** on the leaving-group ability of the parent phenol of the sulfamate (expressed as pK_a); slope: $\beta_{lg} = -1.1 \pm 0.2$ (mean ± ßstandard deviation).

Active-site titration of *Pa*AtsA by sulfamates

We next investigated the stoichiometry of the inactivation of *Pa*AtsA by the simple aryl sulfamates **4**, **9**, and **11**, the potent estrone sulfatase inactivators COUMATE[10] and 667COUMATE,[11] and the novel inactivator FLAVOMATE (flavonol-3-*O*-sulfamate; Scheme 1). COUMATE and 667COUMATE were prepared according to literature procedures.[10,11] FLAVOMATE was prepared by the treatment of flavonol with sulfamoyl chloride in *N*,*N*-dimethylacetamide/acetonitrile (see the Supporting Information). Kinetic analysis revealed that COUMATE, 667COUMATE, and FLAVOMATE are outstandingly potent time-dependent inactivators of *Pa*AtsA, equal in activity to or better than the best simple aryl sulfamates studied (Table 2). As a point of interest, we observed a K_i value of 180 ± 40 nM and a k_{inact} value of $0.24 \pm 0.08\ s^{-1}$ for 667COUMATE with *Pa*AtsA, whereas the corresponding values for the inactivation of estrone sulfatase are $K_i = 40$ nM and $k_{inact} = 0.00345\ s^{-1}$.[11] FLAVOMATE was the most potent inactivator studied; its high rate of inactivation prevented the accurate determination of inactivation parameters.

The following titration method was used to determine residual activity (Figure 5A): A fixed amount of *Pa*AtsA was incubated with the inactivator at various concentrations, and the inactivation reactions were allowed to proceed to completion. After a period sufficient for at least 95% enzyme inactivation ($t_{0.95}$), the residual enzymatic activity was determined by fluorometry with substrate **2**. Additional samples were taken over a period of $4 \times t_{0.95}$ or longer to ensure that complete inactivation had occurred. This titration method does not allow monitoring of the fate of the inactivator after binding to the enzyme; however, unlike the direct titration approach (see below), it imposes no demands in terms of the detection of the inactivator or its decomposition products and uses small amounts of enzyme (as little as 33 nM *Pa*AtsA).

"Direct titration" was performed by assaying spectrophotometrically the amount of phenol released upon extended inactivation of the enzyme (>95% inactivation) by **4** and COUMATE (Figure 5B). Varying amounts of the enzyme were titrated, and the results averaged. This direct method might lead to the overestimation of titration stoichiometry owing to unproductive turnover of the inactivator, that is, turnover that does not result in inactivation, and so the result obtained should always be compared to that of a titration of residual activity. Interestingly, attempts at the direct titration of *Pa*AtsA with FLAVOMATE with spectrophotometric detection of released flavonol gave a nonlinear relationship with increasing amounts of the enzyme. This outcome might be a result of limited flavonol solubility in the aqueous solvent at the relatively high concentrations used (100 μM), which might lead to aggregate formation and, consequently, to nonspecific enzyme inactivation.[29]

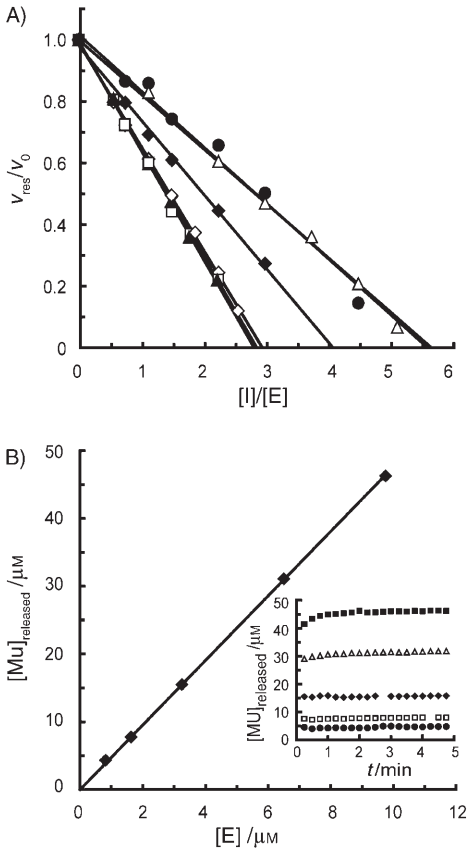

Figure 5. The titration of *Pa*AtsA with aryl sulfamates reveals variable inactivation stoichiometry. A) Residual-activity titration with FLAVOMATE (●), **4** (△), COUMATE (◆), **9** (□), 667COUMATE (▲), and **11** (◇). Inactivation mixtures containing the enzyme and increasing concentrations of the sulfamate were incubated (37 °C, pH 7) until inactivation was complete. Residual hydrolytic activity (v_{res}) was assayed at pH 9 by fluorometry with substrate **2**. The intersection of the plot of v_{res}/v_0 against the inactivator/enzyme ratio ([I]/[E]) with the *x* axis ($v_{res}=0$) reveals the stoichiometry of inactivation. B) Direct titration of *Pa*AtsA with COUMATE. Reaction mixtures containing excess inactivator (100 μM) and increasing concentrations of the enzyme were incubated (37 °C, pH 7) until inactivation was complete. The amount of released 4-methylumbelliferone (MU) was assayed spectrophotometrically. The slope of a plot of released 4-methylumbelliferone [MU] against enzyme concentration [E] allows the calculation of the stoichiometry of inactivation ([I]/[E] = 4.8, $r^2=0.998$). Inset: Time dependence of the release of 4-methylumbelliferone in inactivation mixtures containing the enzyme at concentrations of 9.8 (■), 6.5 (△), 3.3 (◆), 1.6 (□), and 0.81 μM (●).

Alternatively, *Pa*AtsA could be titrated with FLAVOMATE by taking advantage of the ability of the released flavonol to form a highly fluorescent chelate with aluminium(III).[30] Thus, after a period of time sufficient for at least 95% inactivation, the inactivation mixtures containing a constant excess of FLAVOMATE and increasing concentrations of the enzyme were added to excess $AlCl_3$ at pH 4.5. The amount of the fluorescent aluminium chelate of released flavonol ($\lambda_{ex}=400$ nm, $\lambda_{em}=450$ nm) was determined by comparison with a calibration curve. This method allowed the reliable titration of the enzyme at concentrations as low as 181 nM and was highly sensitive even at low concentrations of FLAVOMATE (10 μM). The results of all titration experiments are summarised in Table 3.

Table 3. Stoichiometry of the inactivation of *Pa*AtsA by the sulfamates **4**, **9**, **11**, COUMATE, 667COUMATE, and FLAVOMATE.[a]

Inactivator	k_{inact}/K_i [s^{-1} μM^{-1}][b]	[I]/[E] (residual activity)[c]	[I]/[E] (direct)[d]
11	0.0043 ± 0.0005	3.0	n.d.[e]
9	0.31 ± 0.05	2.8	n.d.[e]
667COUMATE	0.74 ± 0.3	2.9	n.d.[e]
COUMATE	1.0 ± 0.3	4.2	4.8
4	1.1 ± 0.4	5.7	5.8
FLAVOMATE	> 2	5.7	6.0

[a] The ratio [I]/[E] was calculated by using the enzyme concentration determined by GC/MS. [b] The k_{inact}/K_i ratio was determined under titration conditions as described in Table 2. [c] Result of residual-activity titration. [d] Result of direct spectrophotometric or fluorometric titration. [e] Not determined.

Discussion

Aryl sulfamates undergo spontaneous hydrolysis in aqueous solution by an E*l*c*B* mechanism: deprotonation of the nitrogen atom is followed by elimination of the conjugate base to afford $HNSO_2$, which reacts to form various addition products.[31] The spontaneous rate of hydrolysis increases with increasing pH and is inversely proportional to the pK_a value of the parent phenol.[31] Thus, for the maximum stability of aryl sulfamates, inactivation assays should be performed at low pH values. However, *Pa*AtsA is essentially inactive at pH < 5, and at pH 5 aryl sulfamates do not cause time-dependent inactivation of *Pa*AtsA. The lack of inactivation at pH 5 results from the absence of an irreversible step (i.e., $k_{inact}=0$). Others[18,23] observed no reactivation of the closely related estrone sulfatase when inactivated by sulfamates, and Purohit et al. observed that estrone sulfatase could only be inhibited by EMATE at pH > 7.[9] Thus, inactivation assays with *Pa*AtsA were carried out at pH 7, as a compromise between maintaining the ability of sulfamates to inactivate *Pa*AtsA in a time-dependent manner and ensuring sufficient stability of the enzyme to determine kinetic parameters. Under these conditions, only aryl sulfamates with a parent phenol of p$K_a \geq 7.9$ were stable enough to be studied. Surprisingly, others who have attempted to examine the inactivation of sulfatases by aryl sulfamates have ignored this fundamental physical limitation. Thus, the Brønsted plot of inactivation potency versus the pK_a value of the parent phenol reported by Patel and co-workers for estrone sulfatase is fatally flawed.[32] Wong and co-workers interpreted the formation of "a deep yellow solution" during the inactivation of PaAtsA by 4-nitrophenyl sulfamate as evidence for the release of 4-nitrophenol upon inactivation; however, our observation of an uncatalysed hydrolysis rate of 0.08 min^{-1} for this inactivator casts serious doubts on their conclusion.[18]

Table 2 shows inactivation parameters (k_{inact} and K_i) for aryl sulfamates **4**–**12** with varying pK_a values of the parent phenol. Even the poorest inactivators **11** and **12** had low micromolar K_i values, whereas the most potent inactivators exhibited low nanomolar inhibition constants. The efficiency of inactivation can be gauged by examination of the second-order rate con-

stant k_{inact}/K_i. Accordingly, the best inactivator from the aryl sulfamate series, 4-cyanophenyl sulfamate (**4**), is 310 times as efficient as the poorest inactivator studied, 4-methoxyphenyl sulfamate (**12**). Differences in the efficiency of *Pa*AtsA inactivation by aryl sulfamates are best revealed through the presentation of the results as a linear free-energy Brønsted plot of the pK_a value of the parent phenol versus log k_{inact}/K_i (Figure 4). Despite the relatively narrow range of pK_a values (7.97–10.10) of the parent phenols of the compounds studied, this plot shows clearly a strong relationship between the potency of the inactivator and the pK_a value of the parent phenol ($\beta_{lg} = -1.1 \pm 0.2$). The steep slope of this plot and its linear character imply a high degree of charge development in the transition state. This result suggests strongly that the cleavage of the ArO–S bond of the sulfamate is the first irreversible step in the inactivation reaction and, to our knowledge, provides the first direct evidence that the inactivation of sulfatases by aryl sulfamates occurs through this specific chemical step. This conclusion is consistent with the unpublished data reported by Nussbaumer and Billich, who claimed that estrone sulfatase inactivation by EMATE labelled with [^{3}H] on the steroid moiety did not result in radiolabelling of the enzyme.[5]

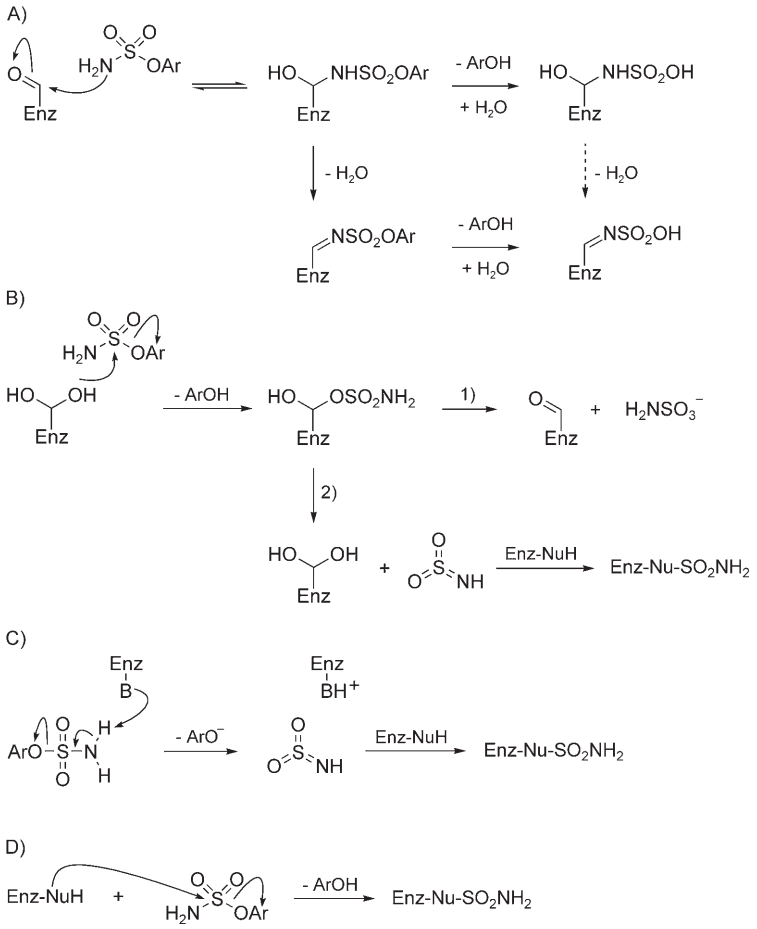

Scheme 3. Proposed mechanisms for the inactivation of *Pa*AtsA by aryl sulfamates.

The scission of the ArO–S bond of an aryl sulfamate during inactivation implies that the stoichiometry of the inactivation process can be measured by quantifying the release of the parent phenol upon reaction with *Pa*AtsA (Figure 5B). The results for **4**, COUMATE, and FLAVOMATE are shown in Table 3. A complementary approach, termed "residual-activity titration", was used to study the same three sulfamates, as well as three other sulfamates derived from poorly chromo-/fluorogenic phenols: **9**, **11**, and 667COUMATE. The residual enzyme activity was measured by the titration of enzyme activity with a substoichiometric amount of the inactivator (Figure 5A). Comparison of the stoichiometry determined from these two titration methods revealed comparable titration results (Table 3). The stoichiometry varied for the different aryl sulfamates, with the ratio [I]/[E] in the range 3–6. Interestingly, more-potent inactivators (with higher k_{inact}/K_i values) gave higher titration results. The observation that more-reactive sulfamates react with a higher inactivation stoichiometry indicates that the stoichiometry-determining step of the inactivation process involves the loss of the phenol leaving group.

Potter and co-workers[10] and Hanson et al.[18] proposed several possible mechanistic alternatives for the inactivation of sulfatases by sulfamates. Our observation of the strong dependence of inactivation efficiency upon the pK_a value of the parent phenol and detection of released phenol upon inactivation provide strong evidence in favour of a mechanism involving scission of the ArO–S bond during the inactivation process. The following alternatives are plausible (Scheme 3): A) The addition of an aryl sulfamate (or its conjugate base) to the aldehyde form of *Pa*AtsA to afford an *N*-alkyl sulfamate ester hemiaminal, followed by the loss of the corresponding phenol derivative, can lead to either an *N*-alkyl sulfamic acid hemiaminal or an iminosulfamic acid; B) S_N2 substitution at the sulfur atom of the aryl sulfamate by the hydrated form of FGly can lead to the expulsion of the parent phenol and formation of an enzyme α-hydroxysulfamate; C) E1*c*B elimination of the sulfamate or its conjugate base can lead to the formation of $HNSO_2$ (possibly with the assistance of a divalent cation in the active site) and its subsequent addition to an active-site nucleophile; finally, D) S_N2 substitution at the sulfur atom of the aryl sulfamate by an active-site nucleophile can lead to a direct transfer of the sulfamoyl group to the nucleophile. Additionally, general base-assisted reactions of the enzyme α-hydroxysulfamate that results from mechanism B might occur: 1) elimination of sulfamic acid to regenerate the aldehyde form of FGly, and subsequent reaction of sulfamic acid with an active-site residue, or 2) elimination of $HNSO_2$, which then reacts according to mechanism C. However, the inactivation of *Pa*AtsA by sulfamic acid formed in (1) is ruled out, because sulfamic acid does not cause detectable inactivation of *Pa*AtsA (data not shown).

Although it is well known that aryl sulfamates react preferentially through an E1*c*B mechanism, such as B1 or C, unsubstituted sulfamates can react through a bimolecular S_N2-type mechanism, such as that shown in D, albeit at low rates.[31] *N*,*N*-Dialkyl sulfamates, which react exclusively through an S_N2

mechanism, are not inactivators of estrone sulfatase.[33] Although this observation could be interpreted to rule out a bimolecular S_N2 reaction in the active site, it is possible that *N*,*N*-dialkyl-substituted sulfamates cannot react with an active-site residue owing to steric factors. Comparison of the slope of the Brønsted plot obtained in this study for the inactivation of *Pa*AtsA ($\beta_{lg} = -1.1$) with that measured for the uncatalysed hydrolysis of aryl sulfamates at pH 7 ($\beta_{lg} = -1.2$) provides circumstantial evidence in favour of a direct elimination mechanism that involves the formation of $HNSO_2$ (mechanism C).[31] The similarity of the two slopes implies similar degrees of charge transfer and similar transition states for the two processes. Unfortunately, however, to the best of our knowledge, the corresponding Brønsted relationship for S_N2 substitution has not been reported. Further support for mechanism C is the observation that the hydrogen atom on the N atom of sulfamates is relatively acidic (for example, the pK_a value of 4-nitrophenyl sulfamate is 7.29).[31] It is likely that at pH 7 all sulfamates studied are present as their conjugate base ($ArOSO_2NH^-$) to a significant extent, whereas at pH 5 only the protonated form is present. The inability of sulfamates to inactivate *Pa*AtsA at pH 5 implies that the conjugate base of the sulfamate is the reactive species required for inactivation, as suggested previously for steroid sulfatase.[11] Alternatively, an acidic active-site residue that is fully protonated at pH 5 might be required for inactivation. The dependence of inactivation on the pH value suggests that mechanism D, which involves nonspecific sulfamoylation of *Pa*AtsA by direct S_N2 reaction at the sulfur atom without the involvement of a general base, is unlikely.

Any mechanistic proposal for the inactivation of sulfatases by aryl sulfamates must be consistent with the variable inactivation stoichiometry observed in this study. As proposed previously,[11] multiple sulfamoylation could occur through specific labelling of a set of reactive residues (possibly by a direct S_N2 mechanism as in D, or through the random sulfamoylation of active-site residues, for example, by the intermediate $HNSO_2$). Disappointingly, our attempts to observe adducts on inactivated *Pa*AtsA by ESIMS were unsuccessful: although *Pa*AtsA ionises efficiently in the mass spectrometer and provides an excellent ion current, no adducts were observed. The strongly acidic conditions used for ESI (formic or trifluoroacetic acid) might result in the cleavage of any adduct.

The simplest explanation for the variable reaction stoichiometry observed is the existence of two reaction processes that occur in parallel. One process (e.g., A or B2) leads to inactivation of the enzyme and is the process detected when inactivation kinetics are measured. A second process, which might be independent of the first, results in either multiple cycles of inactivator turnover (e.g., B1) or the direct sulfamoylation of assorted enzyme residues (e.g., C or D). The variable inactivation stoichiometry, which increases for more reactive sulfamates, suggests that more reactive inactivators are either turned over more times or sulfamoylate more enzyme residues. The first-order nature of enzyme inactivation suggests that mechanism A occurs. Similarly, the pH dependence of inactivation, which does not occur at $pH \leq 5$, suggests that mechanism C is responsible for the nonunity stoichiometry of inactivation. It is quite possible that additional sulfamoylation of an already inactivated enzyme occurs. Such reactions are in effect kinetically invisible, as they are obscured from detection during the measurement of inactivation kinetics; however, they are still measured in the titration experiments. Notably, the inactivation of estrone sulfatase by EMATE,[9] COUMATE,[10] and 667COUMATE[11] occurs with biphasic kinetics, whereby a slower inactivation process occurs after partial inactivation. Thus, multiple sulfamoylation reactions are probably occuring with this closely related enzyme. Nucleophiles of *Pa*AtsA that might undergo sulfamoylation include the *gem*-diol of FGly51 and other conserved nucleophiles in the active site, such as Lys113, His115, His211, and Lys375 (Scheme 4).[14] These residues are equivalent to those suggested for the inactivation of steroid sulfatase by sulfamates.[11]

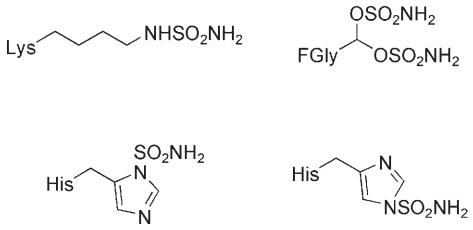

Scheme 4. Structures of possible sulfamoylated active-site residues derived from the sulfamoylation of lysine, histidine, and FGly.

Conclusions

Although aryl sulfamates were described as effective sulfatase inactivators more than a decade ago, and despite the fact that 667COUMATE is in clinical trials as an estrone sulfatase inactivator, their mechanism of action remains obscure. We have studied the bond-breaking steps that occur during inactivation and the stoichiometry of inactivation of a model sulfatase, *Pa*AtsA. On the basis of studies with a range of aryl sulfamates of varying reactivity, we present the first conclusive evidence that the inactivation of sulfatases by aryl sulfamates occurs through cleavage of the ArO–S bond. In support of this conclusion, we observed directly the loss of the phenolic moiety during the inactivation process by photo- and fluorometric techniques. Titration studies revealed a nonunity stoichiometry of inactivation, and the results imply that multiple sulfamoylation reactions occur during inactivation. Our results support the sulfamoylation of the enzymic FGly residue in a reaction that proceeds through an E*l*c*B* mechanism and involves an $HNSO_2$ intermediate. However, other nonspecific enzyme-labelling processes are likely to occur in parallel with specific active-site labelling. The identification of the ultimate dead-end product of inactivation by sulfamates, which might have implications for the potential immunogenicity of sulfamate inactivators when used clinically, has proven to be an extremely challenging task. Structural elucidation of the inactivated form of a sulfatase and detailed kinetic investigations of inactivation stoichiometry by using active-site mutants of *Pa*AtsA are required

to provide further evidence for the identity of the enzyme residue(s) that undergo sulfamoylation.

Experimental Section

General: Spectrophotometric measurements were performed with a Cary-50 Bio UV/Vis spectrophotometer (Varian) equipped with a circulating water bath and 18-cell accessory, in disposable Dynalon UV-grade disposable methacrylate cuvettes with a path length of 1 cm (Sigma–Aldrich). Fluorometric measurements were performed with a Cary Eclipse fluorometer (Varian) in disposable polystyrene cells with a path length of 1 cm (Starna). Buffer A is 25 mM bis-tris propane/25 mM glycine/0.05% bovine serum albumin (BSA); buffer B is 50 mM citric acid/potassium citrate/0.05% BSA; and buffer C is 100 mM potassium phosphate.

Kinetic analysis of *Pa*AtsA: Assays were conducted at 37 °C in buffer A. Kinetic measurements with potassium 4-methoxyphenyl sulfate (**1**) were performed at pH 7 with or without 5% EtOH, or at pH 9. Reactions were performed in triplicate and were initiated by the addition of the enzyme solution with a syringe to a preincubated buffer containing **1** (at seven concentrations, 0.3–12×K_m) to a final enzyme concentration of 41 nM for assays at pH 9 and 81 nM for assays at pH 7. The hydrolysis rate was monitored continuously with a UV/Vis spectrophotometer ($\Delta\varepsilon_{296}=1640\,M^{-1}cm^{-1}$). Kinetic measurements with potassium 4-methylumbelliferone sulfate (**2**) were performed at pH 9. Reactions were initiated by the addition with a syringe of the enzyme solution to a final concentration of 0.41 nM to preincubated buffer containing **2** (at 12 concentrations, 0.02–8×K_m), and the hydrolysis rate was monitored continuously with a fluorescence spectrophotometer (**2**: $\lambda_{ex}=359$ nm, $\lambda_{em}=451$ nm; slit width: 2.5 and 5 nm). Linear rates were analysed by nonlinear regression analysis by using GraFit 4.05 (Erithacus Software Ltd., Surrey, UK) to obtain k_{cat} and K_m values. Comparative activity assays at pH 3, 5, 7, and 9 were performed by adding the enzyme (41 nM) to substrate **1** (3 mM) in buffer A at pH 7 or 9 or buffer B at pH 5 and monitoring the linear hydrolysis rate as above. In stability assays, the enzyme was preincubated for 0–60 min in the respective buffer and assayed in buffer A at pH 9 as described above.

Determination of the K_i value of sodium tetraborate: The K_i value of sodium tetraborate was determined from the initial rate of hydrolysis of **1** in buffer A at pH 9 and 37 °C in the presence of sodium tetraborate. Substrate concentrations spanned from K_m/3 to 3×K_m, and inhibitor concentrations spanned from K_i/3 to 2.5×K_i. Reactions were initiated by the addition of *Pa*AtsA, and the initial rate was monitored at 296 nm. The data obtained were subjected to nonlinear regression analysis by using GraFit. K_i(sodium tetraborate) = 178 ± 14 μM.

***Pa*AtsA inactivation assays**: Each inactivation mixture contained the enzyme (9 nM) in buffer A at pH 7 (285 μL). Inactivation reactions were initiated by the addition of an aliquot (15 μL) of a stock solution of one of the aryl sulfamates **4–12**, COUMATE, 667COUMATE, or FLAVOMATE in EtOH to the preincubated solution of the enzyme. The resulting mixture was incubated at 37 °C in a water bath, and samples (20 μL) were taken every 15–30 s until no enzyme activity was detectable. The samples were then diluted into preincubated buffer A containing substrate **2** (1.98 mL, 30 μM) at pH 9 and 37 °C, and residual enzyme activity was monitored by fluorometry (**2**: $\lambda_{ex}=359$ nm, $\lambda_{em}=451$ nm; slit width: 5 nm). In the control assay, the solution of the sulfamate was replaced with EtOH. Inactivation was stopped by 100-fold dilution into a buffer containing the substrate **2**. The concentration of the sulfamate in the inactivation mixture ranged from 0.1–5×K_i for compounds **7–12** and 0.3–1.6×K_i for compounds **4–6**, COUMATE, and 667COUMATE, with reactions at 7–10 of these concentrations performed in duplicate. The inactivation of *Pa*AtsA by FLAVOMATE was too rapid for the acquisition of reliable data; therefore, only an estimate is presented. Pseudo-first-order rate constants (k) for each inactivator concentration were determined from the slope of the semilogarithmic plot of residual rate, v_{res}, of the hydrolysis of substrate **2** against preincubation time, t, according to Equation (3):

$$\ln(v_{res}/v_0) = -k \times t \quad (3)$$

The k_{inact} and K_i values were obtained by nonlinear regression data analysis by GraFit according to Equation (4), in which [I] is the concentration of the inactivator:

$$k = \frac{k_{inact} \times [I]}{K_i + [I]} \quad (4)$$

The time dependence of inactivation at various pH values at 37 °C was tested at a single concentration of the inactivator phenyl sulfamate (**11**): An inactivation mixture containing the enzyme (1.8 μM) and **11** (20 μM) was incubated in buffer A at pH 7 or 9, or buffer B at pH 5, with 5% EtOH, and aliquots were taken every 30 s until no enzyme activity was detectable. The aliquots were assayed by 50-fold dilution in buffer A at pH 9 containing substrate **1** (3 mM) and preincubated at 37 °C, and the hydrolysis rate was monitored continuously by using a UV/Vis spectrophotometer ($\Delta\varepsilon_{296}=1640\,M^{-1}cm^{-1}$). Semilogarithmic plots were constructed to obtain the respective pseudo-first-order rate constants (k) according to Equation (3).

To assess the protection from sulfamate inactivation of *Pa*AtsA by the competitive inhibitor sodium tetraborate, an inactivation mixture containing the enzyme (1.8 μM), sodium tetraborate (at six concentrations, 0–2 mM), and **11** (20 μM) was incubated in buffer A at pH 9 with 5% EtOH at 37 °C. Samples were taken at regular time intervals and assayed at 296 nm as described above. Residual hydrolysis rates were corrected for the presence of tetraborate in the assay according to Equation (5), in which v_{corr} is the corrected residual rate, v_{app} is the observed residual rate, [I_c] is the assay concentration of sodium tetraborate, K_c is 178 μM, and [S] is the concentration of substrate **1** (3 μM):

$$v_{corr} = v_{app} \times \left(1 + \frac{K_m \times [I_c]/K_c}{K_m + [S]}\right) \quad (5)$$

Pseudo-first-order rate constants (k) were determined according to Equation (3). A plot of inverse pseudo-first-order rate constant (k^{-1}) against tetraborate concentration [I_c] allowed the calculation of the K_i value of the inactivator according to Equation (6), in which $[I_c]_0$ is the tetraborate concentration corresponding to the intersection of the plot with the x axis ($k^{-1}=0$), and [I] is the inactivator concentration (20 μM):

$$K_i = -\frac{K_c \times [I]}{[I_c]_0 + K_c} \quad (6)$$

To study the irreversibility of *Pa*AtsA inactivation by phenyl sulfamate (**11**), the enzyme (6.5 μM) was incubated with **11** (1 mM) in buffer A at pH 7 or 9 without BSA (total volume 1.5 mL) at 37 °C. After 20 min, an activity check (3 mM substrate **1** in buffer A at pH 9) confirmed full enzyme inactivation. The sample was dialysed against buffer A (6×8 mL) by using an Amicon YM-10 centrifugal

ultrafiltration device (Millipore) at 3000 rpm and 4 °C to a final volume of 200–500 μL. Subsequent activity measurement confirmed no recovery of activity. A control sample, without **11**, was treated in the same way with no loss of activity observed. Reactivation of inactivated *Pa*AtsA was tested as follows: A sample of *Pa*AtsA (6.5 μM, 1.5 mL), inactivated at pH 7 as described above, was loaded with a syringe (5 mL min^{-1}) onto a Hi-Trap Desalting column (5 mL, GE Healthcare) equilibrated with buffer B (pH 5) without BSA. The enzyme was eluted at 4 °C in one fraction (1 mL) after a void volume (1.5 mL). The enzyme was incubated at pH 5 for 1 h at 37 °C. During this period, aliquots were assayed for activity (3 mM substrate **1** in buffer A at pH 9). No recovery of activity was observed. The control sample maintained activity during purification but lost substantial activity after 1 h at 37 °C in a buffer at pH 5.

Active-site titration by residual-activity assay: Inactivation mixtures containing the enzyme (163 nM) and **4**, **9**, COUMATE, 667COUMATE, or FLAVOMATE (at ten concentrations (0–5 μM), at seven of which nonzero residual activity was observed) were incubated in buffer A at pH 7 with 5% EtOH at 37 °C. Samples were taken after 1, 3, 5, 7, 9, and 11 min of incubation, diluted 100-fold into buffer A (pH 9) containing substrate **2** (30 μM), and assayed by fluorometry (λ_{ex} = 359 nm, λ_{em} = 451 nm; slit width: 2.5 nm). For samples taken after 3–11 min, a time period of $\geq t_{0.95}$ to $\geq 4 \times t_{0.95}$ had elapsed. The time required for at least 95% inactivation of the enzyme ($t_{0.95}$) for **9**, the slowest inactivator in the series, was 153 s at 94 nM, the lowest concentration used. The residual hydrolysis rate (v_{res}/v_0) was plotted against the ratio of the concentrations of the inactivator and the enzyme [I]/[E], and the intersection of the plot with the *x* axis ($v_{res} = 0$) revealed the inactivation stoichiometry.

A higher enzyme concentration (325 nM) and longer incubation times (1.5–6.5 h) were used for the assays of inactivator **11** (13 concentrations, 0–5 mM) as a result of its low k_{inact}/K_i value ($t_{0.95}$ = 187 min at 63 nM, the lowest concentration used).

Active-site titration by measurement of the amount of released phenol: Reaction mixtures containing sulfamate **4** or COUMATE (100 μM) and *Pa*AtsA (at five concentrations, 0.81–9.8 μM) were incubated in buffer B at pH 7 with 5% EtOH at 37 °C, and the amount of released chromophore was monitored by UV/Vis spectrophotometry for 5 min (at pH 7; $\Delta\varepsilon_{270} = 4100\ M^{-1}cm^{-1}$ and $\Delta\varepsilon_{340} = 9100\ M^{-1}cm^{-1}$ for **4** and COUMATE, respectively) to ensure that the absorbance remained constant after 1 min ($\geq t_{0.95}$). An inactivator blank (enzyme substituted by a buffer) and a protein blank (sulfamate substituted by EtOH) were treated analogously and used to correct the experimental value. The concentration of the phenol released in each inactivation mixture was plotted against the enzyme concentration. The slope of the line of best fit afforded the inactivation stoichiometry.

For FLAVOMATE, the quantity of released flavonol was determined by detection of the fluorescent aluminium chelate formed by the addition of aluminium(III) to flavonol.[30] Inactivation mixtures (300 μL) containing FLAVOMATE (10 μM) and the enzyme (0.18–0.81 μM) were incubated in buffer A at pH 7 with 5% EtOH at 37 °C. After 1 min ($\geq t_{0.95}$), the inactivation mixture was added to a mixture of $AlCl_3$ in water (0.01 M) and buffer B at pH 5 (2:3, final pH value: 4.5). The chelate was allowed to develop (4 min) and was quantified by fluorometry (λ_{ex} = 400 nm, λ_{em} = 450 nm; slit width: 10 nm) by comparison with a calibration curve. The value found for the sample was corrected against the fluorescence of a reaction blank (with the enzyme substituted by a buffer). The concentration of the chelate formed in each inactivation mixture was plotted against the enzyme concentration, with the slope of the plot indicating the inactivation stoichiometry.

Acknowledgements

This research was supported by grants from the Australian Research Council (DP0449625), the Selby Foundation, The University of Melbourne, and Sterix Ltd., a member of the Ipsen Group. ED is supported by a Sir John and Lady Higgins Research Scholarship; M.J.M. is a National Health and Medical Research Council Principal Research Fellow.

Keywords: enzyme catalysis · inhibitors · kinetics · reaction mechanisms · structure–activity relationships

[1] K. G. Bowman, C. R. Bertozzi, *Chem. Biol.* **1999**, *6*, R9–R22.
[2] M. A. Kertesz, *FEMS Microbiol. Rev.* **2000**, *24*, 135–175.
[3] S. R. Hanson, M. D. Best, C.-H. Wong, *Angew. Chem.* **2004**, *116*, 5858–5886; *Angew. Chem. Int. Ed.* **2004**, *43*, 5736–5763.
[4] M. J. Reed, A. Purohit, L. W. Woo, S. P. Newman, B. V. L. Potter, *Endocr. Rev.* **2005**, *26*, 171–202.
[5] P. Nussbaumer, A. Billich, *Med. Res. Rev.* **2004**, *24*, 529–576.
[6] J. A. Hoffman, J. L. Badger, Y. Zhang, S. H. Huang, K. S. Kim, *Infect. Immun.* **2000**, *68*, 5062–5067.
[7] J. D. Mougous, R. E. Green, S. J. Williams, S. E. Brenner, C. R. Bertozzi, *Chem. Biol.* **2002**, *9*, 767–776.
[8] A. Ratzka, H. Vogel, D. J. Kliebenstein, T. Mitchell-Olds, J. Kroymann, *Proc. Natl. Acad. Sci. USA* **2002**, *99*, 11223–11228.
[9] A. Purohit, G. J. Williams, N. M. Howarth, B. V. L. Potter, M. J. Reed, *Biochemistry* **1995**, *34*, 11508–11514.
[10] L. W. L. Woo, A. Purohit, M. J. Reed, B. V. L. Potter, *J. Med. Chem.* **1996**, *39*, 1349–1351.
[11] L. W. L. Woo, A. Purohit, B. Malini, M. J. Reed, B. V. L. Potter, *Chem. Biol.* **2000**, *7*, 773–791.
[12] S. J. Stanway, A. Purohit, L. W. Woo, S. Sufi, D. Vigushin, R. Ward, R. H. Wilson, F. Z. Stanczyk, N. Dobbs, E. Kulinskaya, M. Elliott, B. V. L. Potter, M. J. Reed, R. C. Coombes, *Clin. Cancer Res.* **2006**, *12*, 1585–1592.
[13] S. Beil, H. Kehrli, P. James, W. Staudenmann, A. M. Cook, T. Leisinger, M. A. Kertesz, *Eur. J. Biochem.* **1995**, *229*, 385–394.
[14] I. Boltes, H. Czapinska, A. Kahnert, R. von Bulow, T. Dierks, B. Schmidt, K. von Figura, M. A. Kertesz, I. Uson, *Structure* **2001**, *9*, 483–491.
[15] T. Dierks, B. Schmidt, L. V. Borissenko, J. Peng, A. Preusser, M. Mariappan, K. von Figura, *Cell* **2003**, *113*, 435–444.
[16] Q. Fang, J. Peng, T. Dierks, *J. Biol. Chem.* **2004**, *279*, 14570–14578.
[17] F. G. Hernandez-Guzman, T. Higashiyama, W. Pangborn, Y. Osawa, D. Ghosh, *J. Biol. Chem.* **2003**, *278*, 22989–22997.
[18] S. R. Hanson, L. J. Whalen, C.-H. Wong, *Bioorg. Med. Chem.* **2006**, *14*, 8386–8395.
[19] C. S. Bond, P. R. Clements, S. J. Ashby, C. A. Collyer, S. J. Harrop, J. J. Hopwood, J. M. Guss, *Structure* **1997**, *5*, 277–289.
[20] G. Lukatela, N. Krauss, K. Theis, T. Selmer, V. Gieselmann, K. von Figura, W. Saenger, *Biochemistry* **1998**, *37*, 3654–3664.
[21] K. J. Loft, S. J. Williams in *Glycobiology*, 1st ed. (Eds.: C. Sansom, O. Markman), Scion, Bloxham, **2007**.
[22] R. von Bulow, B. Schmidt, T. Dierks, K. von Figura, I. Uson, *J. Mol. Biol.* **2001**, *305*, 269–277.
[23] L. C. Ciobanu, R. P. Boivin, V. Luu-The, F. Labrie, D. Poirier, *J. Med. Chem.* **1999**, *42*, 2280–2286.
[24] E. Denehy, J. M. White, S. J. Williams, *Chem. Commun.* **2006**, 314–316.
[25] R. Kitz, I. B. Wilson, *J. Biol. Chem.* **1962**, *237*, 3245–3249.
[26] R. Recksiek, T. Selmer, T. Dierks, B. Schmidt, K. von Figura, *J. Biol. Chem.* **1998**, *273*, 6096–6103.
[27] M. Okada, S. Iwashita, N. Koizumi, *Tetrahedron Lett.* **2000**, *41*, 7047–7051.
[28] P. M. Laidler, J. Steczko, *Acta Biochim. Pol.* **1986**, *33*, 101–108.

[29] J. Seidler, S. L. McGovern, T. N. Doman, B. K. Shoichet, *J. Med. Chem.* **2003**, *46*, 4477–4486.
[30] E. H. Jackim, R. I. Saunderstown, D. B. Land, *Phosphate Derivatives of 3-Hydroxyflavone*, USA 3,453,291, **1969**.
[31] S. Thea, G. Cevasco, G. Guanti, A. Williams, *J. Chem. Soc. Chem. Commun.* **1986**, 1582–1583.
[32] S. Ahmed, C. P. Owen, K. James, C. K. Patel, M. Patel, *Bioorg. Med. Chem. Lett.* **2001**, *11*, 899–902.
[33] N. M. Howarth, A. Purohit, M. J. Reed, B. V. L. Potter, *J. Med. Chem.* **1994**, *37*, 219–221.
[34] O. S. Wolfbeis, E. Fuerlinger, H. Kroneis, H. Marsoner, *Fresenius Z. Anal. Chem.* **1983**, *314*, 119–124.
[35] L. Costantino, G. Rastelli, M. C. Gamberini, J. A. Vinson, P. Bose, A. Iannone, M. Staffieri, L. Antolini, A. Del Corso, U. Mura, A. Albasini, *J. Med. Chem.* **1999**, *42*, 1881–1893.
[36] B. G. Tehan, E. J. Lloyd, M. G. Wong, W. R. Pitt, J. G. Montana, D. T. Manallack, E. Gancia, *QSAR* **2002**, *21*, 457–472.

Received: October 1, 2007
Published online on February 20, 2008

